

PAPER • OPEN ACCESS

An analysis research of terrain correction methods considering the slope ranges based on OLI image

To cite this article: Ying Zhang *et al* 2019 *IOP Conf. Ser.: Mater. Sci. Eng.* **592** 012163

View the [article online](#) for updates and enhancements.



IOP | ebooks™

Bringing you innovative digital publishing with leading voices to create your essential collection of books in STEM research.

Start exploring the **collection** - download the first chapter of every title for free.

An analysis research of terrain correction methods considering the slope ranges based on OLI image

Ying Zhang^{1,2*}, Lin Wang¹, Yunfei Ai¹, Xuejiao Bai¹

¹ China Transport Telecommunications & Information Center, Beijing 100011, China

² School of Forestry, Beijing Forestry University, Beijing 100083, China

Corresponding author: august12@163.com

Abstract. In mountainous terrain, the topographic correction often be used in image pre-processing. Recently, some correction approaches considering slope ranges have been developed to improve topographical effects. The paper explores the C correction and Minnaert methods considering the slope ranges to evaluate if the methods considering slope ranges can effectively reduce the topographic effects. The C model constants and Minnaert constants in different slope range were obtained based on the image samples. Then, the scatterplots were used to evaluate the correction results. The model constants analysis shows that the Minnaert constant has a nonlinear relation with slope. The scatterplots analysis shows that the image reflectance using a single correction constant value has a better correction result. When the slopes are greater than 43 degrees, the Minnaert model considering slope has overcorrected the topographic effects. The study has demonstra-ted the Minnaert correction models considering slope range did not better reduce topographic effects and the method need be improved, especially in the high slope ranges.

1. Introduction

Topographic correction in mountainous regions is an important step for classification study and quantitative analysis study. The shadows resulting from deep slope and lush vegetation often happen in mountainous regions. It is necessary to apply optimal methods to reduce the topographic effects for accurate quantitative remote sensing information acquisition.

Many approaches have been developed to correct the topographic effects [1-4]. The statistical models [5, 6] include the Teillet-regression correction method and the b correction method. The C correction model and Minnaert model are the frequently used in topographic correction. The C correction model was developed by improving the physical cosine model [3]. Riano has assessed different methods for topographic correction of Landsat Thematic Mapper images and the C model obtained the best result [7]. The Minnaert-correction model makes use of a Minnaert constant k , which depends on the nature of land-cover, topographic factor, and wavelength. Recently, some researchers proposed that the model coefficient should be computed in different slope ranges. The coefficients considering slope ranges can improve the accuracy of terrain correction. For example, Lu has developed a pixel-based Minnaert coefficient image based on the established relationship between Minnaert coefficients and topographic slopes and select different Minnaert k coefficients based on the slope range [8]. Huang has tested the slope-based method and obtain better topographic correction results [9]. The different C-correction strategies, including different NDVI intervals, different land use types, and different slope intervals, were used to eliminate the effects of topography on Landsat TM



images in complex mountains [10]. And the result found no uniform method for all bands to achieve the best correction results [10].

Some studies have shown that topographic correction methods considering slope has improved topographic correction result. However, the method is no universal topographic correction approach. In the article, by comparing the topographic correction results based on C model and Minnaert model considering slope range, we explored the effectiveness of the topographic correction considering the slope range. we used Landsat 8 Operational Land Imager (OLI) image as experiments and performed scatterplots analysis to evaluate the topographic correction results.

2. Materials and methods

2.1. The study area

The study area is located in Jiangle County, Fujian province, China (Figure 1). Digital elevation model (DEM) data with 30 m spatial resolution and a Landsat-8 Operational Land Imager (OLI) image (path/row: 120/041), which was acquired on 17 October 2014 cloud-free were used in this research. The solar azimuth and elevation angles were 150.639 and 49.183 degrees, respectively. Firstly, the OLI image was Radiometric Calibration, which the OLI DN (Digital Numbers) were converted to at-sensor reflectance with an apparent reflectance model by ENVI tools. Then, the OLI image was rectified with 23 control points which were collected from the corrected Worldview-2 image with high spatial resolution. The root mean square error (RMSE) was 0.3877 pixels.

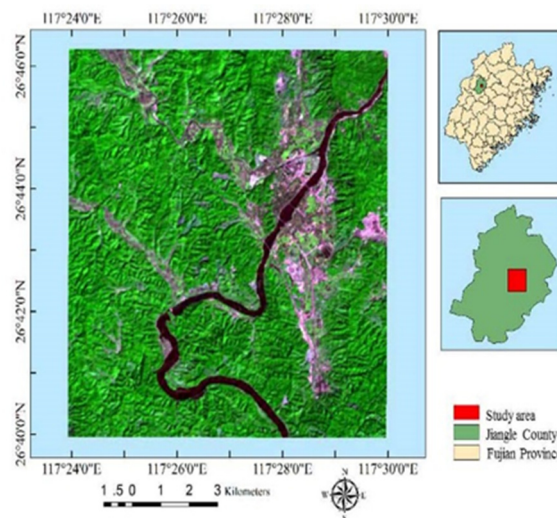


Fig.1 Study area: Jiangle County, Fujian province, China.

2.2. The Methods of Terrain Correction

This paper compares the topographic correction methods considering the slope in mountainous terrain. Based on the following equations, the solar zenith angle, azimuth, slope and aspect are the required parameters used in C-correction and the Minnaert correction model. The slope and aspect images can be obtained by computing DEM data. The azimuth and solar zenith angle are from the ETM metadata. Then, the illumination can be computed by the parameters with the equation 2. The ETM image, illumination and slope images are then stacked into one file by ENVI tools. Sample data are extracted from the entire image on the stacked file.

2.2.1. *The C-correction Model.* The C-correction model can be expressed as Equation 1:

$$\rho_H = \rho_T (\cos \theta_z + C_\lambda) / (\cos \gamma_i + C_\lambda) \quad (1)$$

Where the C_λ is correction coefficient. The ρ_H is the equivalent reflectance on a flat surface with incident angle of zero. ρ_T is the measured radiance in the remotely sensed data. θ_z is solar zenith angle. The cosine of the incident solar angle ($\cos \gamma_i$), referred to as illumination, is calculated using Equation 2:

$$\cos \gamma_i = \cos \theta_p \cos \theta_z + \sin \theta_p \sin \theta_z \cos(\varphi_\alpha - \varphi_0) \quad (2)$$

Where γ_i is the solar incident angle in relation to the normal of a pixel. θ_p and φ_0 are slope and aspect of the terrain. θ_z and φ_α are solar zenith angle and azimuth angle.

The correction coefficient C_λ calculated using Equation 3:

$$\rho_T = \alpha_\lambda + b_\lambda \cos \gamma_i, \quad C_\lambda = \alpha_\lambda b_\lambda^{-1} \quad (3)$$

Where $\alpha_\lambda, b_\lambda$ is the empirical coefficients of optical band.

2.2.2. The Minnaert Correction Model. The Minnaert correction model can be expressed as Equation 4:

$$\rho_H = \rho_T \cos \theta_p / (\cos \theta_p \cos \gamma_i)^k \quad (4)$$

The Equation 4 can be reorganized as Equation 5 to solve k:

$$\log(\rho_T \cos \theta_p) = \log(\rho_H) + k \log(\cos \theta_p \cos \gamma_i) \quad (5)$$

2.3. Topographic Correction Coefficients

The samples with slopes are divided into 10 groups based on the slope ranges. A regression analysis is conducted for each slope group based on Equation 3 and 5. Then the C_λ and k value can be developed for each ETM band corresponding to each slope group. The equation (3) indicates that the C_λ is equivalent to the ratio of intercept to slope of a regression equation. The equation (5) indicates that the k is equivalent to the slope of a regression equation.

3. Results

3.1. The Correction Coefficients Analysis

As Figure 2 shows, the C correction coefficients value is no relation to slope. However, the Minnaert correction coefficient k value is wavelength-dependent and relation to slope. The Minnaert k values increases when the wavelength increases. For example, the band 7 has highest Minnaert k values and the band1 has lowest Minnaert k values at the same slope. In addition, the Minnaert k value shows a similar trend for each band. When the slope increases, the Minnaert k values decrease. For all bands, the Minnaert k correction coefficients decrease rapidly between 1 and 15 degrees. And then the k values become stable in the slope ranges of 15 to 30 degrees. For band1 to band4, the k values decrease slightly when the slopes are greater than 30 degrees. However, for band5, band6 and band7, the k values show an obviously decrease when the slopes are greater than 30 degrees. The analysis confirms that, for an entire image, a single global Minnaert k value is not suitable. The trend of k values versus slope can be simulated using polynomial regression for each band, and the coefficients of determination (R^2) are greater than 0.9 for each band.

3.2. Scatterplot for Correction Result Image

Figure 3 displays scatter plots and linear regression fitting lines of reflectance versus cosi for OLI band 5 before and after topographic correction. The sub-scene (b) and (c) show the results based on topographic correction methods using a single coefficient. The sub-scene (d) and (e) show the results based on topographic correction methods considering the slope ranges. The correction methods using a single coefficient show a better correction result. The Minnaert correction considering slope range obtains the lowest coefficients of determination (R^2).

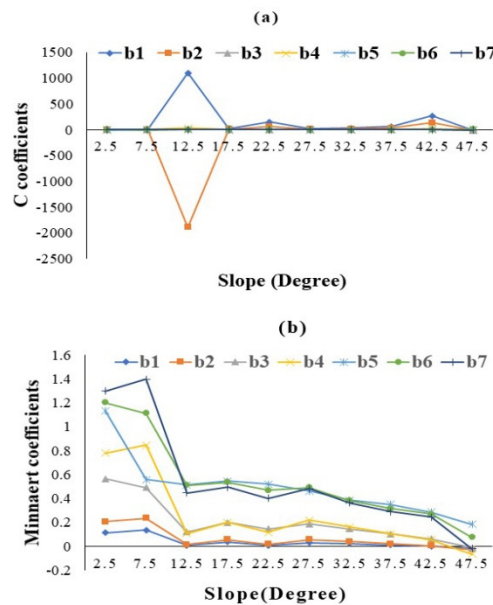


Fig.2 The correction coefficients from topographic correction models considering slope range. (a)C correction model corresponding to the slope; (b)Minnaert model corresponding to the slope.

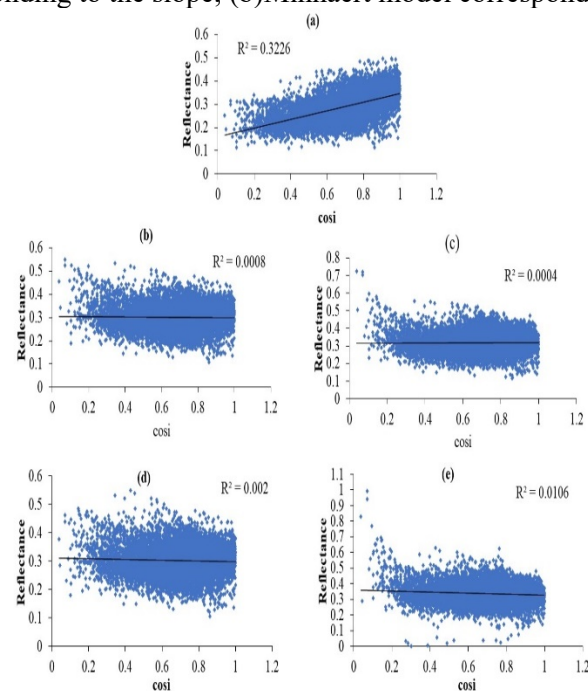


Fig.3 Scatter plots and linear regression fitting lines of reflectance versus $\cos i$ for OLI band 5 before and after correction. (a) original image; (b) C-correction result using a single correction value; (c) Minnaert correction result using a single correction value; (d) C correction result considering slope range; (e) Minnaert correction result considering slope range.

The figure 4 shows scatter plots and linear regression fitting lines of the reflectance versus slope before and after Minnaert correction. The reflectance is over-corrected when the slopes are greater than 43 degrees. So, for the areas with very high slopes, the impacts of topographic conditions on the remotely sensed data have not been corrected.

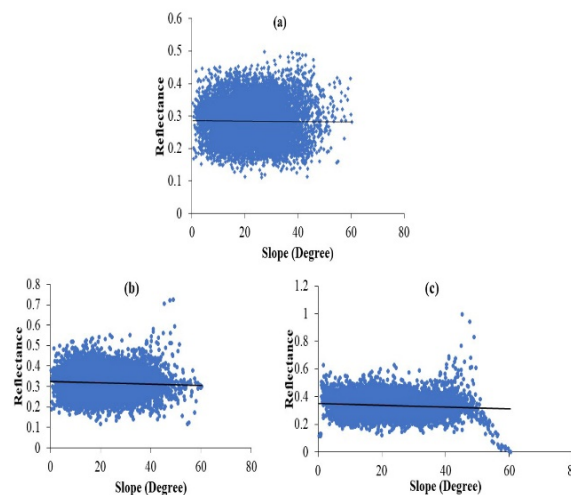


Fig.4 Scatter plots and linear regression fitting lines of reflectance versus slope for OLI band 5 before and after Minnaert correction. (a)original image; (b)Minnaert correction; (c)Minnaert correction considering slope range.

4. Conclusions

The comparison of topographic correction results by different topographic correction methods found that the Minnaert method considering the slope did not obtain the better topographic correction result. The Minnaert constant has a nonlinear relation with slope. However, in high slope ranges, the over-correction phenomenon is serious. The Minnaert method considering the slope need be improved in high slope areas.

Acknowledgment

This work was financially supported by the China Transport Telecommunication & Information Center reserve project in 2018 (2018CB09) and the National Key Research and Development Program of China (2017YFC0803900). The author would like to express thanks to anonymous reviewers and the editors for their remarks.

References

- [1] Gitas I Z, Devereux B J 2006 *International Journal of Remote Sensing* **27**(1) 41-54
- [2] Yu Z X, Zhang C, Chen J Z 2017 *Journal of Southwest Forestry University* **37**(6) 178-187
- [3] Gao M L, Zhao W J, Gong Z N, Gong H L, Chen Z, Tang X M J R S 2014 *Remote Sensing* **6**(4) 3141-3151
- [4] Wu J, Bauer M E, Dong W, Manson S M J I J O P 2008 *Isprs Journal of Photogrammetry* **63**(2) 223-236
- [5] Teillet P M, Guindon B, Goodenough D G J C J O R S 1981 *J Canadian Journal of Remote Sensing* **8**(2) 84-106
- [6] Vincini M, Frazzi E, Reeder D 2002 *IEEE International Geoscience & Remote Sensing Symposium*
- [7] Riaño D, Chuvieco E, Salas J, Aguado I 2003 *IEEE Transactions on Geoscience & Remote Sensing* **41**(5) 1056-1061
- [8] Lu D, Ge H, He S, Xu A J P E 2008 *Photogrammetric Engineering* 74(11) 1343-1350
- [9] Huang B 2012 *Remote Sensing Technology and Application* 27(2) 183-189
- [10] Li C C, Fan J C, Fu X H, Fan H 2014 *Journal Of Geo-Information Science* 16(1) 134-141